Chapter 3: Pre-Stack Predictive Multiple Suppression

3.1 Introduction

The 1960's saw the development of very sophisticated one-dimensional theories for multiple reflection (Goupillaud (1961), Sherwood and Trorey (1965), and Treitel and Robinson (1966)). The failure of these sophisticated models to lead to practical results consistently better than predictive deconvolution led in the 1970's to increasing attention to the spatial aspects of the problem. Taner (1980) (also Harms, personal communication) began by addressing the problem of offset with a radial trace theory. Riley (1976) introduced migration operators to vertical wave stacks to handle the effects of dip. Estevez (1977) extended Riley's results to slant stacks to incorporate the wider offsets found in practice.

Both Riley and Estevez applied their wave theories to stacks, unlike the present thesis. Plane wave stacking improves signal to noise and may have been essential considering the computer power of the time. In retrospect, the results of Chapter 1 & 2 illustrate the importance of attacking multiples on unstacked data.

The goal of this chapter is to develop a pre-stack theory of predictive multiple suppression valid for all angles of dip and offset. This goal is attained in Section 3.3 with the derivation of a multiple dereverberation operator valid for all water bottom and pegleg multiples. A full implementation of this operator is very costly because of its extreme generality. Nevertheless, it serves as a useful tool in understanding some of the prominent predictive methods used in industry.

3.2 Replacement Medium Concept of Multiple Suppression

The concept of a "replacement medium" is used extensively in the geophysical literature. A well known example can be found in the study of gravity. In computing the Bouger gravity anomaly, the actual density distribution in the crust is conceptually replaced to some datum level by a uniformly dense slab. The Bouger anomaly is then computed relative to this replacement medium. In this particular case, we are trying to simulate a zone of uniform impedance to a datum just below the seafloor. This is consistent with the objective of making the seafloor transparent to seismic illumination. The residual "anomalies" remaining from this process will be either primaries or (low amplitude) intrabed multiples.

In order to obtain further insight, we will digress briefly to explain the concepts of "upcoming/downgoing" and "shot/geophone" wavefields. Everyone has an intuitive idea of what is meant by upcoming and downgoing waves. Mathematically, these terms are well defined only if velocity is z-variable or constant. The question of direction then depends on the choice of sign for the z-component of the propagation vector, **k** , when the dispersion relation is factored. *I.e.* - Direction depends on the sign of

$$\partial_z = \pm \frac{i\omega}{v(z)}\sqrt{1 - (\frac{vk_x}{\omega})^2} \qquad (3.2.1)$$

For media with laterally varying velocity we cannot make this definition. In practice, however, this does not stop us from assigning the labels "upcoming" and "downgoing" to wavefields. Provided we restrict ourselves to smoothly varying velocity distributions and ignore waves with very high propagation angles, the notion of "upcoming" and "downgoing" wavefields seems to be well enough defined.

Under the common assumption of two-dimensional symmetry, the seismic data collected in a field experiment is a function of five variables - two spatial variables for shot location, another two for geophone location, and one for time or frequency. A "geophone" wavefield denotes a wavefield obtained by fixing the shot coordinates and allowing the receiver coordinates to vary. A "shot" wavefield is a wavefield for which the opposite is true.

The pre-stack multiple suppression problem is one of the few areas of exploration seismology where all four wavefield combinations (upcoming/downgoing and shot/geophone) must be considered simultaneously. In contrast, post (slant) stack multiple attenuation uses two wavefields - one upcoming and one downgoing (Estevez, 1977). Conventional migration only uses the upcoming geophone wavefield (since the experiment is zero-offset and the "explosive reflectors" concept is invoked).

Let's return now to the concept of a replacement medium. The observed data is given as a surface wavefield - downgoing in shot coordinates and upcoming in geophone coordinates (Fig. 3.2.1). An important intermediate goal will be to *simulate the seismic response of a downgoing shot wavefield and an upcoming receiver wavefield - both just below the seafloor.* This is consistent with our final goal of simulating a transparent sea floor since this can be obtained from the intermediate wavefield by upward continuing shots and receivers from the sea floor datum to the sea surface.

Let's examine what this involves in more detail. The wave equation and the boundary conditions at the sea surface and the sea floor provide all the necessary equations. Since the pressure at the surface vanishes, the upcoming wave, U, is the negative of the

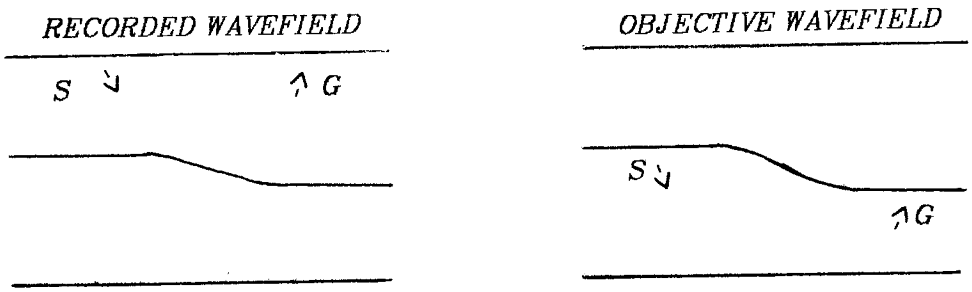

FIG. (3.2.1). The observed data (left) can be thought of as a surface wavefield - downgoing in shot and upcoming in geophone coordinates. Simulating a transparent seafloor requires that both these wavefields lie beneath the seafloor.

downgoing wave, D, at $z=0$. Now consider what happens at the seafloor, $z=z_f$. We define the symbols $\overline{U}$ and $\underline{U}$ to mean upcoming wavefields just <u>above</u> and just <u>below</u> the seafloor. If c is the reflectivity, and t the transmissivity of the seafloor, we have (Fig. 3.2.2) that

$$\overline{U} = t\,\underline{U} + c\overline{D} \tag{3.2.2}$$

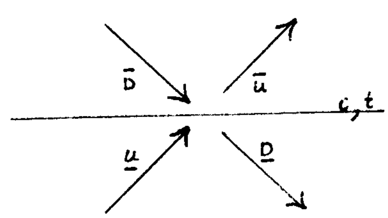

FIG. (3.2.2). $\overline{U} = t\,\underline{U} + c\overline{D}$

Ignoring transmission effects then gives a boundary condition of

$$\underline{U} = \overline{U} - c\overline{D} \tag{3.2.3}$$

First note that in order to apply the boundary condition at the seafloor, $z = z_f$, we need to have access to both $\overline{U}$ and $\overline{D}$ at that depth. Fortunately, because of the surface boundary condition, the observed data gives us both the upcoming and the downgoing wavefields at $z = 0$. The basic steps in achieving our goal can now be stated.

(1) Downward continue the known upcoming and downgoing geophone wavefields (common shot gathers) from the surface to the seafloor. This is done separately for each different shot location.

(2) Apply the seafloor boundary condition, $\underline{U} = \overline{U} - c\overline{D}\,|_{z=z_f}$, to obtain an upcoming geophone wavefield just below the seafloor.

(3) Upward continue the wavefield of Step 2 back through the water (as if the seafloor wasn't there) in order to tie the primaries and residual multiples to the original data. (This is what is meant by the term "replacement medium" in this section heading).

Let's now direct our attention to Figure 3.2.3. From this figure we see that any pegleg which bounces *after* going into the sub-surface would have to be recorded in the surface geophone wavefield before executing that bounce. Such a multiple would be predicted in step one. In fact, the effect of Steps 1-3 is to suppress all water bottom multiples and most pegleg multiples. The only remaining pegleg multiples have raypaths which undergo all of their seafloor bounces before going into the sediments.
To eliminate these remaining multiples, it is necessary to get the downgoing shot wavefield below the seafloor. This is accomplished in the next step by appealing to seismic reciprocity.

(4) Interchange shots and geophones. In practice this amounts to sorting the data into "common geophone gathers" from the field data. Reciprocity tells us that the upcoming receiver wavefields now become downgoing shot wavefields, and vice-versa. In doing this we have automatically solved the problem of getting the downgoing shot wavefield through the seafloor. Admittedly, we have created a fresh problem (the problem of getting the new upcoming geophone field under the seafloor). This, however, is a problem we have already solved in the first three steps.

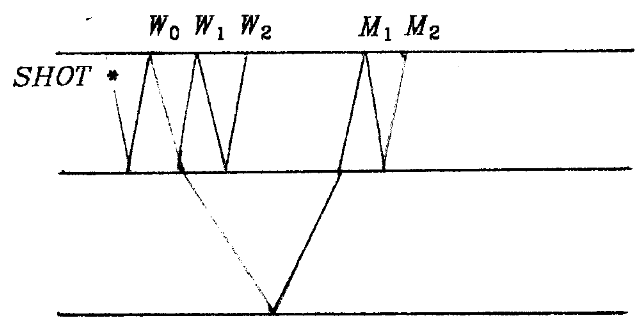

FIG. (3.2.3). All water bottom multiples $W_1, W_2, \ldots$ are predicted from events $W_0, W_1, \ldots$ on the geophone wavefield. Pegleg multiples $M_2, M_3, \cdots$ are also predicted from events $M_1, M_2, \ldots$ on the geophone wavefield. The multiple M_1, however, cannot be predicted from any event in the surface geophone wavefield. It must be predicted, instead, from the shot wavefield.

(5) Repeat steps 1-3, but with the common geophone gathers (shot wavefields) instead of the common shot gathers.

3.3 Wave Equation Multiple Prediction

The last section presented the general concepts involved in suppressing wide-angle marine multiples. This section will build some mathematical structure into these ideas.

Section 3.2 argued that multiple suppression begins by downward continuing all the geophone wavefields or "common shot gathers". Consider, then, the problem of predicting the seafloor reverberations from a single such field experiment (Figure 3.3.1). The total pressure, P, recorded by the hydrophones near the surface is the sum of an upcoming wave, U, and a downgoing wave, D. We'll decompose U and D into a sequence of reverberation subfields, U_i and D_i, with

$$U = \sum_{i=0}^{\infty} U_i \tag{3.3.1a}$$

and

$$D = \sum_{i=0}^{\infty} D_i \tag{3.3.1b}$$

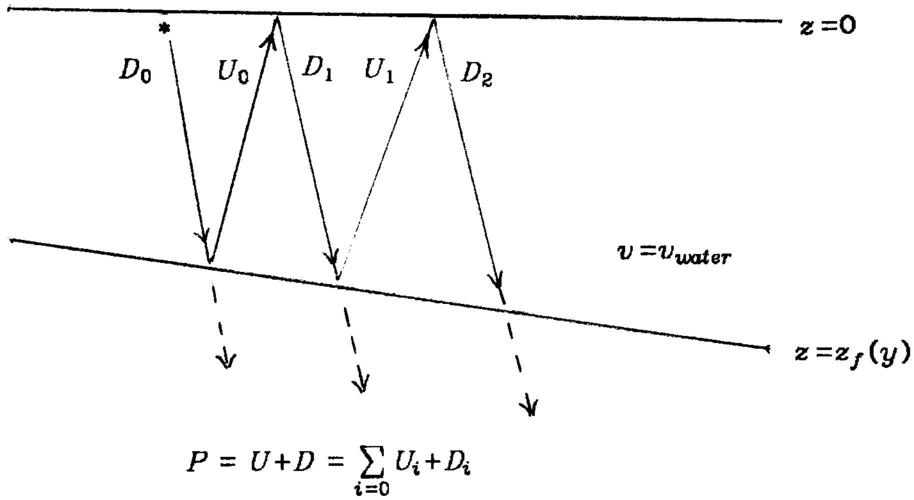

FIG. (3.3.1). Decomposition of upcoming and downgoing wavefield in water layer.

We impose the boundary condition that $D_i = -\nu_g U_{i-1}$ at $z = d_g$, the depth of the geophones. In the absence of complications, $\nu_g = 1$. More generally, ν_g accounts for geophone ghosting effects - including a possibly imperfect reflection coefficient at the sea-surface. The upcoming wavefield reflected from the seafloor at $z = z_f$ is $U_i = c_g D_i$. The linear operator, c_g, accounts for seafloor reflectivity. Note that ν_g,c_g,d_g, and z_f can be space variable. We have not yet specified the mathematical parameterization of ν and c - we have merely said that they are linear operators. If they are space-invariant, then both their parameterization and computation simplify greatly.

Let $\downarrow_g$ and $\uparrow_g$ denote linear operators for the one way wave equation in the water. The operator, $\downarrow_g$, will serve to propagate a <u>downgoing</u> wavefield in geophone coordinates from $z=d_g$ to $z=z_f$. We define $\uparrow_g$ as the operator which takes an <u>upcoming</u> geophone wavefield from $z=z_f$ to $z=d_g$. Note that $\downarrow_g$ and $\uparrow_g$ are both diffraction operators. They differ in the specification of their boundary conditions. $\downarrow_g$ terminates at the seafloor whereas $\uparrow_g$ begins there. (If z_f and d_g are constant horizontally, then $\downarrow_g = \uparrow_g$ by symmetry). These relations are summarized in equations 3.3.2-3.3.5.

$$D_i \,|_{z=d_g} = -\nu_g \, U_{i-1} \,|_{z=d_g} \tag{3.3.2}$$

$$D_i \,|_{z=z_f} = \downarrow_g D_i \,|_{z=d_g} \tag{3.3.3}$$

$$U_i \,|_{z=z_f} = c_g D_i \,|_{z=z_f} \tag{3.3.4}$$

$$U_i \,|_{z=d_g} = \uparrow_g U_i \,|_{z=z_f} \tag{3.3.5}$$

Equations 3.3.2-3.3.5 give the result

$$U_i = -\uparrow_g c_g \downarrow_g \nu_g \, U_{i-1} \,|_{z=d_g} \tag{3.3.6}$$

or (using 3.3.1a)

$$U \,|_{z=d_g} = \sum_{i=0}^{\infty} (-\uparrow_g c_g \downarrow_g \nu_g)^i \, U_0 \,|_{z=d_g} = (1 + \uparrow_g c_g \downarrow_g \nu_g)^{-1} \, U_0 \,|_{z=d_g} \tag{3.3.7}$$

This analysis has ignored the reverberations in the vicinity of the shotpoints. To predict them we appeal to reciprocity and equation 3.3.7. The total wave equation dereverberation operator, $\Delta_{W.E.}$, is the product of the shot and geophone dereverberation operators - just as for the Split-Backus model. In particular, the reverberation-free reflected wavefield near the sea-surface is

$$U_0 = \Delta_{W.E.} \, U \tag{3.3.8}$$

where

$$\Delta_{W.E.} = (1 + \uparrow_s c_s \downarrow_s \nu_s)(1 + \uparrow_g c_g \downarrow_g \nu_g) \tag{3.3.9}$$

Equation 3.3.9 is of considerable theoretical interest, since it shows how wave continuation operators, seafloor reflectivity, and array responses must be manipulated if we wish to suppress multiples to all angles in offset and dip.

The reflectivity, c, and possibly, ν, must be estimated from the seismic data in any practical suppression technique. Although we can measure the seafloor's ultrasonic depth very accurately, our knowledge of its effective seismic depth and reflection character are usually not good enough to deterministically suppress multiples. One of the strengths of the "seafloor-consistent" method of Chapter Two was that it automatically estimated the seafloor's depth and character.

Let's examine equation 3.3.9 in more detail. This equation is of the form

$$\Delta_{W.E.} = [1 + Op(s)]\,[1 + Op(g)] \qquad (3.3.10)$$

Using reciprocity we can also write this as

$$\Delta_{W.E.} = [1 + Op(g)]\,[1 + Op(s)] \qquad (3.3.11)$$

The commutivity rule expressed in equations 3.3.10 and 3.3.11 is interesting but does not really say as much as we would like. The main stumbling block to direct implementation of 3.3.9 is the fact that the unknown seafloor reflection operators do not, in general, commute with the deterministic wavefield continuation or "arrow" operators. The Split Backus model of Chapter One made the simplifying assumption that $\downarrow_s = \uparrow_s = Z^{s/2}$, $\downarrow_g = \uparrow_g = Z^{g/2}$, and $\nu_s = \nu_g = 1$. (The Backus model itself makes the additional assumption that $\uparrow_s = \uparrow_g$). This allowed us to isolate the wave prediction algorithm from the seafloor reflectivity estimation procedure. Ideally, we would like to do the same thing in a more general case.

In Section 3.2 we pointed out that most of the multiples (all the seafloor multiples and n of the n+1 branches of an n'th order pegleg multiple) are removed simply by making the seafloor transparent to the geophones. This corresponds to implementing only the right hand bracket of equation 3.3.9. All of the techniques we'll examine in the remainder of this chapter use this approximation.

3.4 Pre-Stack/Post-Stack Multiple Suppression

It is interesting at this point to examine the main differences between replacement medium pre-stack techniques and the Riley/Estevez post-stack approach. We first note that post-stack methods only require consideration of two wavefields - one upcoming and one downgoing. These wavefields can be expressed in either shot or geophone coordinates - depending on which coordinate has not been stacked out.

Post-stack methods, as proposed by Riley and Estevez, demand that the two wavefields be downward continued to maximum primary depth - applying the previously discussed boundary condition, $\underline{U} = \overline{U} - c\overline{D}$, at each level in z. The output is an image of the primary reflectivity structure, $c(x,z)$.

Finding $c(x,z)$ is a considerably more ambitious goal than the goal embodied in the replacement medium concept of Section 3.2. It involves the problems of multiple suppression, source waveform deconvolution, and migration - all at once. The replacement medium approach attempts to isolate the first problem from the last two.

The downward continuation of Riley and Estevez requires a knowledge of the velocity structure everywhere in the section. Such knowledge is usually not available a-priori, except for the water layer. The dereverberation operator (Equation 3.3.9) concedes this fact. It says that if we are willing to work with all four wavefields, then our ignorance of subsurface velocities need not hurt us.

3.5 Radial Trace Multiple Suppression

We'll now review some of the more common "wave-predictive" multiple suppression methods under the unifying view of the dereverberation operator of Section 3.3. All of these methods have been designed to work in the domain of wide offset and zero dip. The main difference among these various techniques lies in how the arrow propagation operators are approximated. The first such method is called radial trace multiple suppression.[1]

A radial trace (Taner, 1980) is a trace sampled along a trajectory of constant offset/time from a seismic profile. This method of multiple suppression is based on the fact that, for a flat seafloor, water bottom multiples on a common shot gather have a reverberation time that is a function of their radial angle only (Figure 3.5.1). For a water column of two way vertical traveltime, τ, this delay is equal to $\tau \sec\vartheta$ where ϑ is the selected radial angle. All of the arrow propagation operators in equation 3.3.9 are approximated by this single delay operator for radial trace prediction. If the earth were of constant velocity and zero dip, then along a radial trace, all multiples would would mimic the zero offset, zero dip model. Under these conditions, radial trace time delay constitutes a simple method of downward continuation. For a depth-variable velocity earth, however, the pegleg multiples on a radial trace cannot be expected to have the same characteristic reverberation times as the seafloor multiples. Figure 3.5.2 demonstrates this fact.

Figure 3.5.2 shows an attempt to predict water bottom and pegleg multiples by delaying radial traces by the amount $\tau \sec\vartheta$. A synthetic seismogram was created for a model of a water layer of 0.5 seconds over a subsurface reflector at 2.0 seconds. The second layer has an interval velocity of 9000 ft/sec. Radial traces were sampled up to a maximum angle of 25^0. (The reconstructed gather is truncated at this angle). Each of these radial traces was then delayed by 0.5 $\sec\vartheta$ seconds and subtracted from the non-delayed radial trace. The angle here is defined to be the ray angle in the water layer. Figure 3.5.2 is the Cartesian coordinate reconstruction of all the radial space difference traces. Note that while the seafloor multiples (at 1.0 and 1.5 sec.) are correctly predicted, the *pegleg* multiple

(1) Seiscom-Delta trademark is "RAMS".

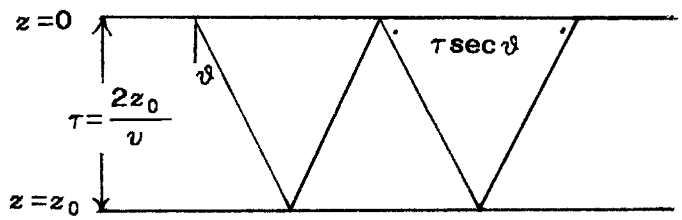

FIG. (3.5.1). The reverberation time for water bottom multiples is $\tau \sec \vartheta$ - a function of angle only.

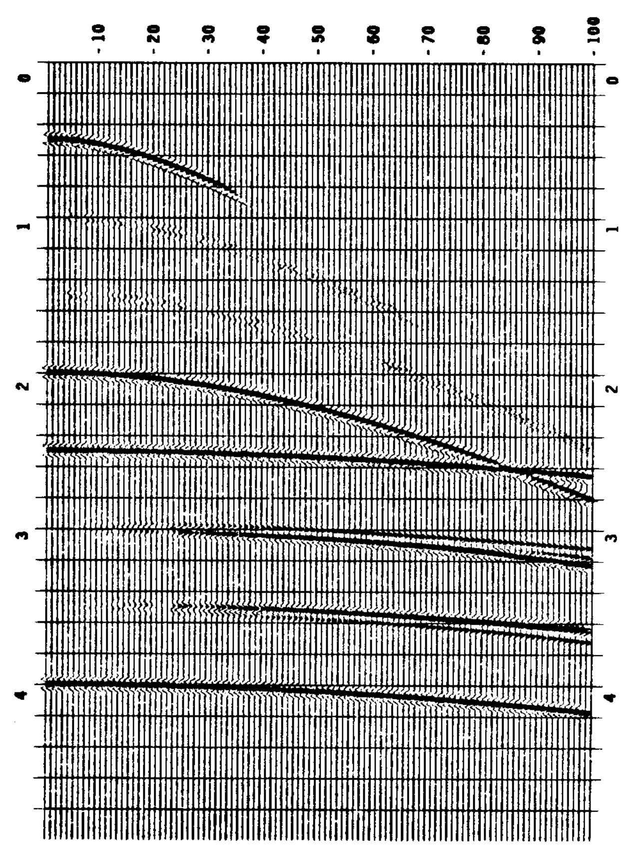

FIG. (3.5.2). Attempt to suppress water bottom and pegleg multiples by delaying and subtracting radial traces in a two layer model. Seafloor multiples (1.0 and 1.5 seconds) are correctly predicted. Pegleg multiples (3.0 and 3.5 seconds) are not well predicted because the sediment velocity differs from water velocity.

predictions (at 3.0 and 3.5 sec.) are out by 50-100 msec. - even at modest offsets.

3.6 Zero Dip - Variable Velocity Multiple Suppression

A better approximation to equation (3.3.9) which overcomes the constant velocity restriction of radial trace prediction has been proposed by Fourmann et al. (1979). To explain this method within the context of equation (3.3.9) we first note that for a flat seafloor of depth d, the propagation operators reduce to simple multiplicative factors in the frequency-wavenumber domain. In particular,

$$\uparrow_s = \downarrow_s = exp(i\frac{\omega}{v}d\sqrt{1-S^2}) \tag{3.6.1}$$

and

$$\uparrow_g = \downarrow_g = exp(i\frac{\omega}{v}d\sqrt{1-G^2}) \tag{3.6.2}$$

where $S = vk_s/\omega$, $G = vk_g/\omega$, v is water velocity and k_s, k_g are the Fourier duals of shot and receiver horizontal coordinates.

We now do something that at first seems unnecessarily complicating, but will lead to simplification. We multiply the left bracket of equation 3.3.9 by the identity operator, $\downarrow_g\downarrow_g{}^{-1}$ and the right bracket by $\downarrow_s\downarrow_s{}^{-1}$. This yields

$$\Delta_{\text{W.E.}} = (1 + \downarrow_g\uparrow_s c_s\downarrow_s\downarrow_g{}^{-1}\nu_s)(1 + \downarrow_s\uparrow_g c_g\downarrow_g\downarrow_s{}^{-1}\nu_g) \tag{3.6.3}$$

This is legitimate since $\downarrow_s$ and $\downarrow_s{}^{-1}$ commute with c_g, the seafloor coupling operator in geophone coordinates and $\downarrow_g$ and $\downarrow_g{}^{-1}$ commute with c_s. The operators in equations 3.6.1 and 3.6.2 can be transformed to dip and offset (Y,H) space by the relations, (Yilmaz, 1979)

$$S = Y + H \tag{3.6.4}$$

$$G = Y - H \tag{3.6.5}$$

Y and H are defined by, $Y = vk_y/2\omega$, $H = vk_h/2\omega$, where k_y and k_h are Fourier duals of midpoint, y and half-offset, h. Now substituting equations (3.6.4) and (3.6.5) into (3.6.1) and (3.6.2) give the relations

$$\downarrow_g\uparrow_s = \downarrow_s\uparrow_g = \exp[i\frac{\omega}{v}d(\sqrt{1-(Y+H)^2} + \sqrt{1-(Y-H)^2}] \tag{3.6.6}$$

and

$$\downarrow_g\downarrow_s{}^{-1} = exp[i\frac{\omega}{v}d(\sqrt{1-(Y-H)^2} - \sqrt{1-(Y+H)^2}] \tag{3.6.7}$$

Expanding the square root arguments of $\downarrow_s \uparrow_g$ and $\downarrow_g \downarrow_s{}^{-1}$ gives

$$\sqrt{1-(Y+H)^2}+\sqrt{1-(Y-H)^2} = 2\sqrt{1-H^2}[1-\frac{Y^2}{2(1-H^2)^2}+O(Y)^4\,] \tag{3.6.8}$$

and

$$\sqrt{1-(Y+H)^2}-\sqrt{1-(Y-H)^2} = \frac{2HY}{\sqrt{1-H^2}}+O(Y)^3 \tag{3.6.9}$$

In the limit of zero dip, (Y=0), equations (3.6.6) and (3.6.8) imply that

$$\downarrow_s \uparrow_g = exp(\frac{2i\omega d}{v}\sqrt{1-H^2}) \tag{3.6.10}$$

Similarly, equations (3.6.7) and (3.6.9) give

$$\downarrow_g \downarrow_s{}^{-1} = 1 \tag{3.6.11}$$

This means that for small dip, (neglecting ghost responses), either one of the brackets in equation 3.6.3 can be implemented by applying the <u>single</u> diffraction operator, $\downarrow_s \uparrow_g$ ($=\downarrow_g \uparrow_s$), to each common midpoint gather and taking the residuals between the diffracted and original gathers. Since $\downarrow_g \downarrow_s{}^{-1}$ and $\downarrow_s \downarrow_g{}^{-1}$ are identity operators in the limit of zero dip, $\Delta_{\not{W}.E.}$ can be much cheaper to implement than equation 3.3.9 might originally suggest.

An example of this process is shown in Figure 3.6.1. This example uses the same model as in Figure 3.4.2. Both the seafloor and pegleg multiples are now properly predicted.

It is interesting to note from equation 3.6.5 that the above scheme could be extended to first order in dip by implementing the operator, $\downarrow_g \downarrow_s{}^{-1}$, as a time and offset dependent midpoint shift. This could be done by approximating H in the space-time domain as $\hat{H} = 2h/vt$. The expression for the phase of $\downarrow_g \downarrow_s{}^{-1}$ in equation 3.6.9 then becomes

$$\frac{2\hat{H}Y}{\sqrt{1-\hat{H}^2}} + O(Y)^3$$

which represents a (time and offset dependent) midpoint shift.

3.7 : Example - Common Shot Gather Multiple Suppression

This section shows some practical results obtained by approximating the dereverberation operator of equation 3.3.9 with its right half only. In particular, we consider the operator

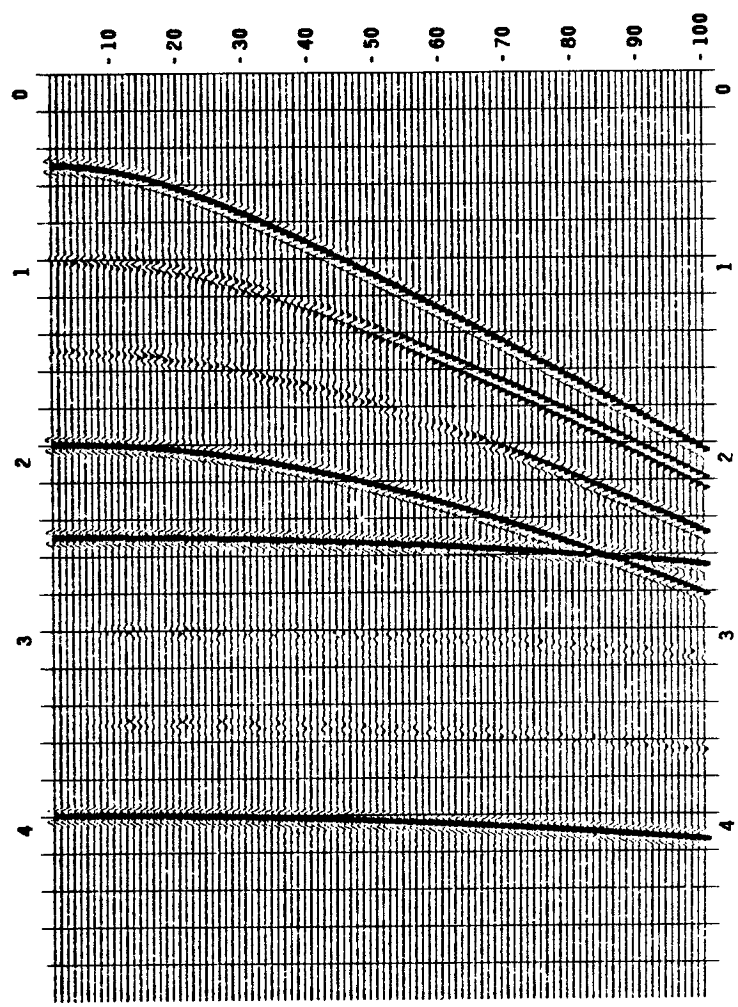

FIG. (3.6.1). Suppression of multiples by the zero dip method for the same model as Figure 3.4.2. A prediction image of the multiples was created by F-K continuation of the surface data to the seafloor. Both seafloor and pegleg multiples are now well predicted. High dip segments of the seafloor multiples are not well cancelled since dip filtering of the prediction image is required to attenuate edge artifacts.

$$\Delta_g = (1 + \downarrow_g c_g \uparrow_g \nu_g) \qquad (3.7.1)$$

We make two additional approximations. The first one is to set $\nu_g = 1$. The second is to allow c_g to commute with $\downarrow_g$. The reflectivity is estimated in the time domain as the shaper filter which minimizes the L_2 error between the observed wavefield, D, and the wavefield, $\downarrow_g \uparrow_g D$. Since the bottom is flat in this example, $\downarrow_g \uparrow_g$ is given by

$$\downarrow_g \uparrow_g = \exp(i\omega\tau\sqrt{1-(\frac{vk_g}{\omega})^2}) \qquad (3.7.2)$$

where τ is the reverberation time of a vertically incident plane wave.

Spatial aliasing and boundary truncation phenomena are always a problem when wave operators are applied to discrete, finite datasets. F-K methods are no exception. Figures 3.7.1 to 3.7.3 will show how some of these practical difficulties were overcome.

Figure 3.7.1 is a common shot gather from the Norwegian Barents Sea. Four water bottom multiples are readily apparent. There are some primaries but they are very difficult to detect pre-stack. The first operation consisted of linear interpolation of the data in NMO coordinates. Data extrapolation was performed by simply replicating the two outermost traces and applying a linear taper from the original data boundary out to the new edge (Fig. 3.7.2). Inverse NMO was then performed to obtain Figure 3.7.3. Although some of the events in Fig. 3.7.3 clearly have jump-slope discontinuities at their suture zones, the strongest amplitude events (water bottom multiples) are correctly extended. It is better to extend the weaker events with an incorrect slope than to simply truncate them.

Figure 3.7.4 is the result of F-K diffracting the dataset in Fig. 3.7.3. No edge effects are apparent. Wraparound was avoided by zero-padding Fig. 3.7.4 to twice its width. Figure 3.7.5 shows two common shot gathers before and after multiple suppression. Some additional event enhancement was obtained by rejecting high negative dips before designing the shaper filters. This explains the absence of the "zippered" texture quality from the multiple-suppressed section.

Figures 3.7.6 and 3.7.7 are the NMO-stacks of the original and multiple-suppressed sections. The earliest event is the direct arrival. The water bottom begins at 600 msec. There are two strong dipping primaries - one at 1.5-1.8 seconds - the other at 3.8-4.1 seconds. Both have pegleg multiple trains associated with them which have been suppressed in the processed stack. After multiple suppression we see a hint of some primaries dipping to the right from the left edge of the section between 2 and 3 seconds.

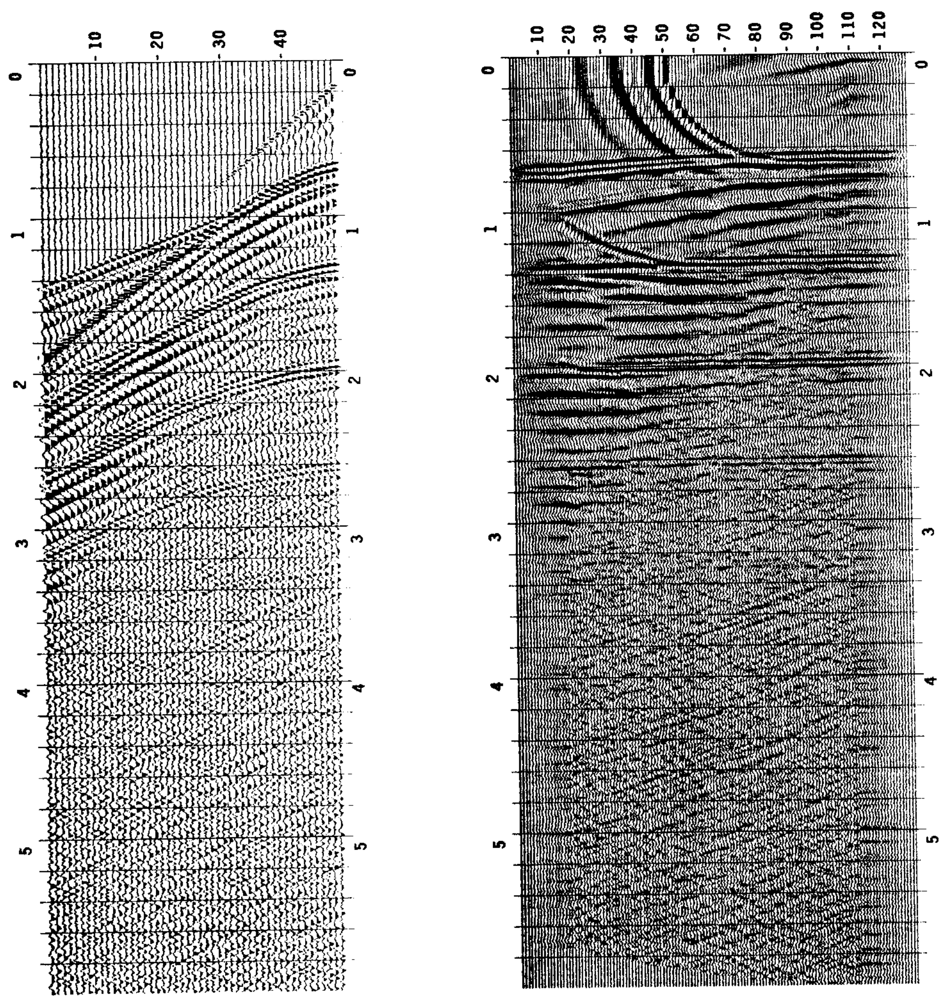

FIG. (3.7.1). (left) Common shot gather - Barents Sea. Fig. (3.7.2) (right) Extrapolated and interpolated gather in NMO coordinates. NMO done at water velocity.

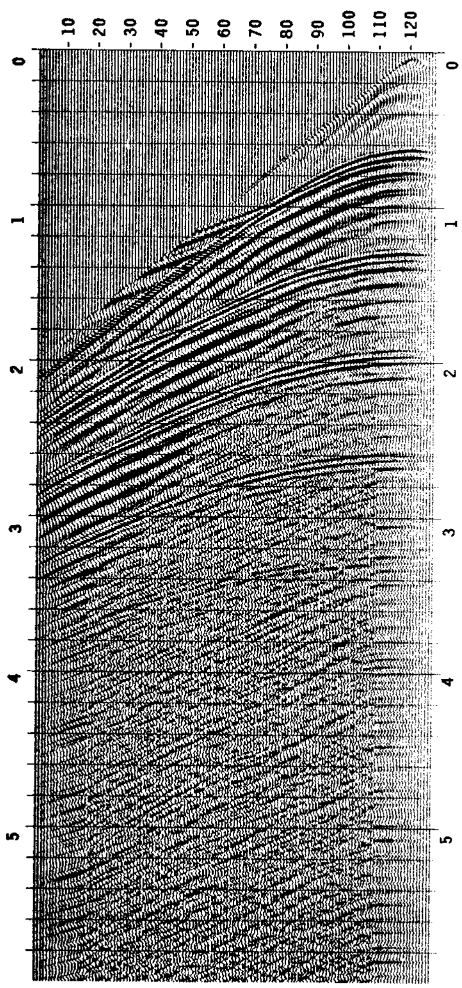

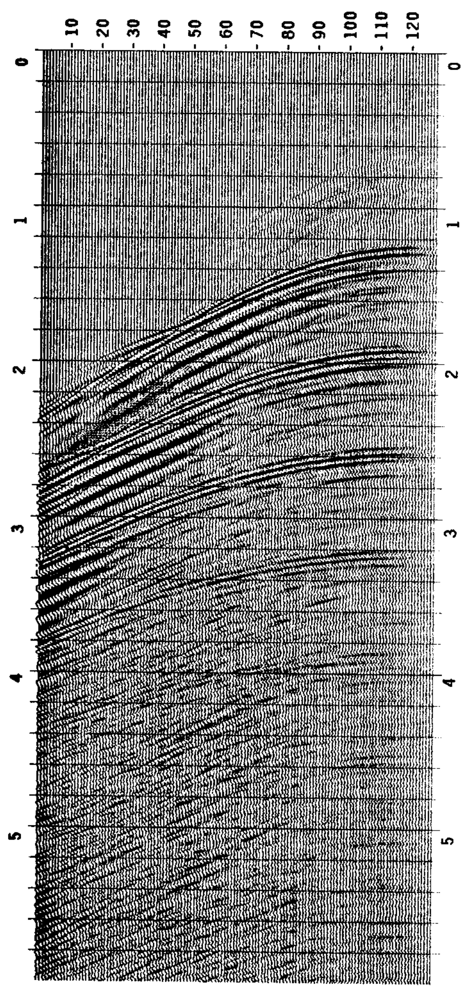

FIG. (3.7.3). (left) Inverse NMO gather from Figure 3.7.2. Fig. (3.7.4) (right) F-K diffracted and dip-filtered version of Figure 3.7.3.

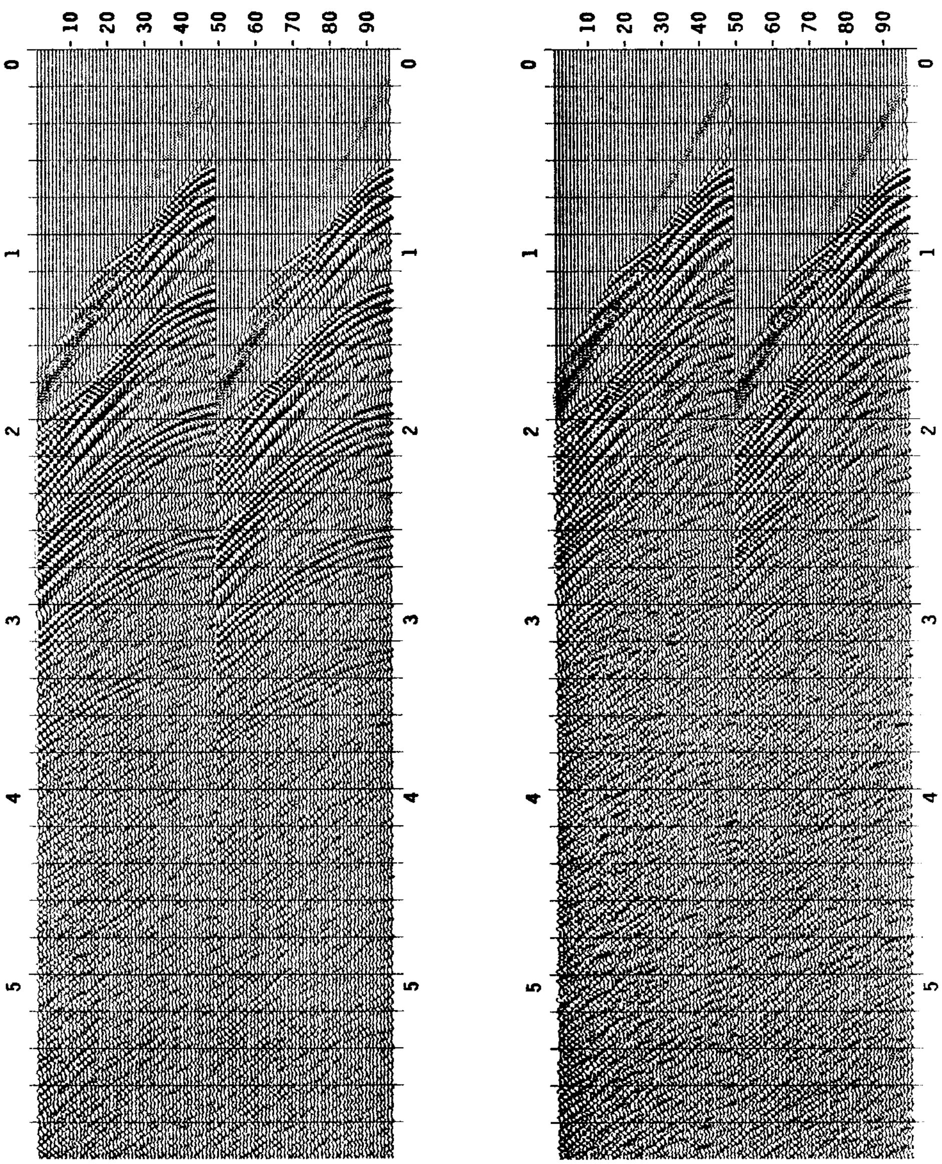

FIG. (3.7.5). Two consecutive gathers - before and after multiple suppression.

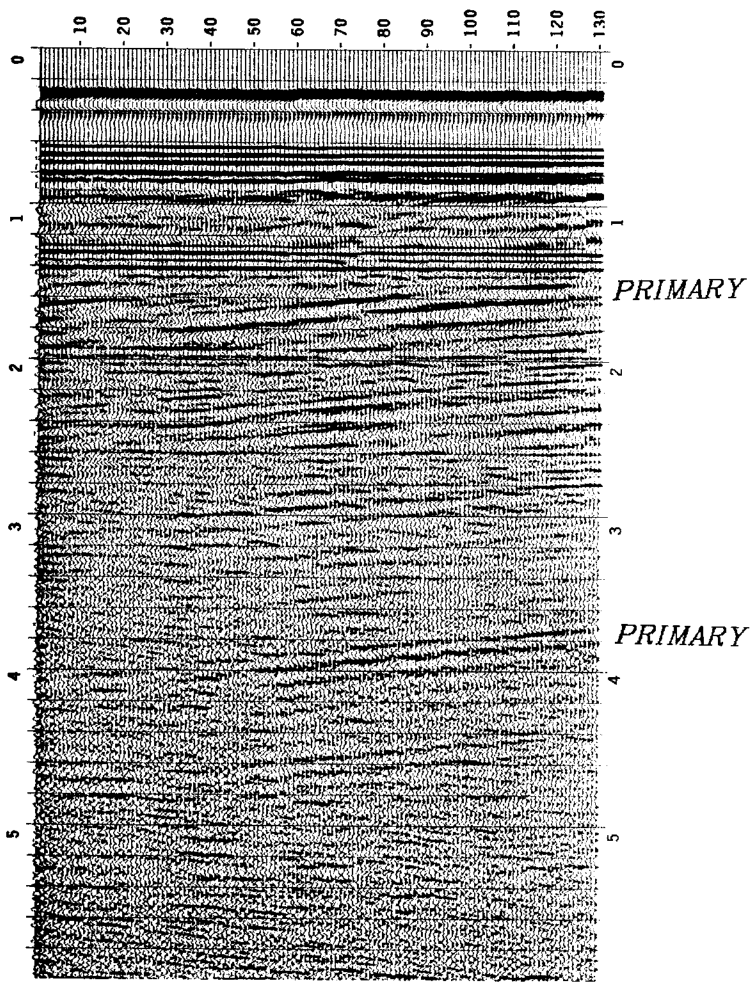

FIG. (3.7.6). NMO-stack - before multiple suppression.

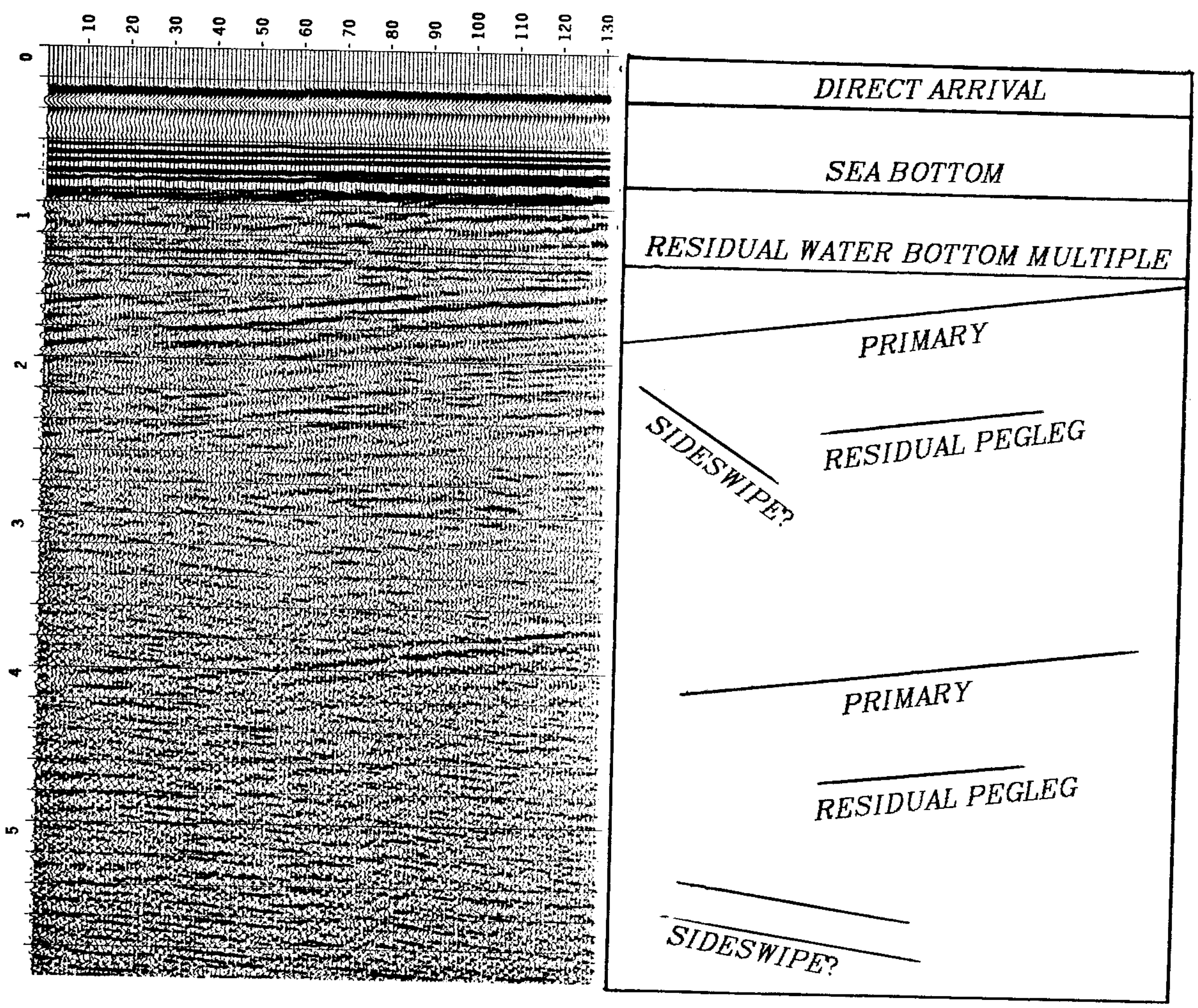

FIG. (3.7.7). NMO-stack - after multiple suppression.

3.8 Slant Stack Multiple Suppression

A third approach to predictive multiple suppression for flat dip and wide offset data uses slant stacks (p-gathers) as input. The underlying principle for this method is the fact that slant stacks preserve the uniformity of the multiple reverberation period. Figure 3.8.1 illustrates this geometrically.

The four hyperbolae in Figure 3.8.1 represent the primary and pegleg reflections for the ray paths shown to their left. The lines EA, FD, $E'A'$ and $F'D'$ have all been constructed tangent to arrivals with common slowness, p_0. The distance, $|AC| = |A'C'|$, since both of these lines represent the two-way traveltime of a ray of constant ray parameter, p_0, through the top layer. The horizontal excursion of this ray in the top layer is $|CD| = |C'D'|$. Now, $<ACD = <A'C'D' = 90°$, $|CD| = |C'D'|$ and $<BDC = <B'D'C'$. This means that triangles BCD and $B'C'D'$ are similar and, in turn, that $|AB| = |A'B'| = |EF| = |E'F'|$. This gives us our claimed result - the slant stack preserves multiple reverberation times for a flat-layered earth. Similar principles can be used to extend the result to a model with any number of flat layers.

Performing a slant stack fixes the ray parameter, p, which is equivalent to fixing S or G in equations 3.6.1 and 3.6.2. This means that the arrow operators for any particular p-trace of a $p-\tau$ gather are pure time delays. If we assume that c and ν are functions of angle rather than space, then c and ν commute with the wave propagation operators. In this case the brackets of equation 3.3.9 can be implemented with trace by trace predictive deconvolution or any other one-dimensional theory.

To the author's knowledge, few applications of this slant stack technique to real data have met with any real success. This seems surprising since the method should be capable of handling the angle dependence of ghost and mud-layer responses. It does this, however, by neglecting all but the most smooth variations in seafloor reflectivity. We might speculate from this that, for most real data, it is better to ignore the angle-dependent rather than the space-dependent effects of the seafloor.

3.9 Summary

In this chapter we derived a multiple dereverberation operator valid for wide angles in both offset and dip. A complete application of this operator to a seismic dataset is equivalent to simulating the upcoming geophone response to a downgoing source field with both sources and geophones placed below the seafloor. The operator combines the effects of wavefield propagation, seafloor reflectivity, and ghost responses.

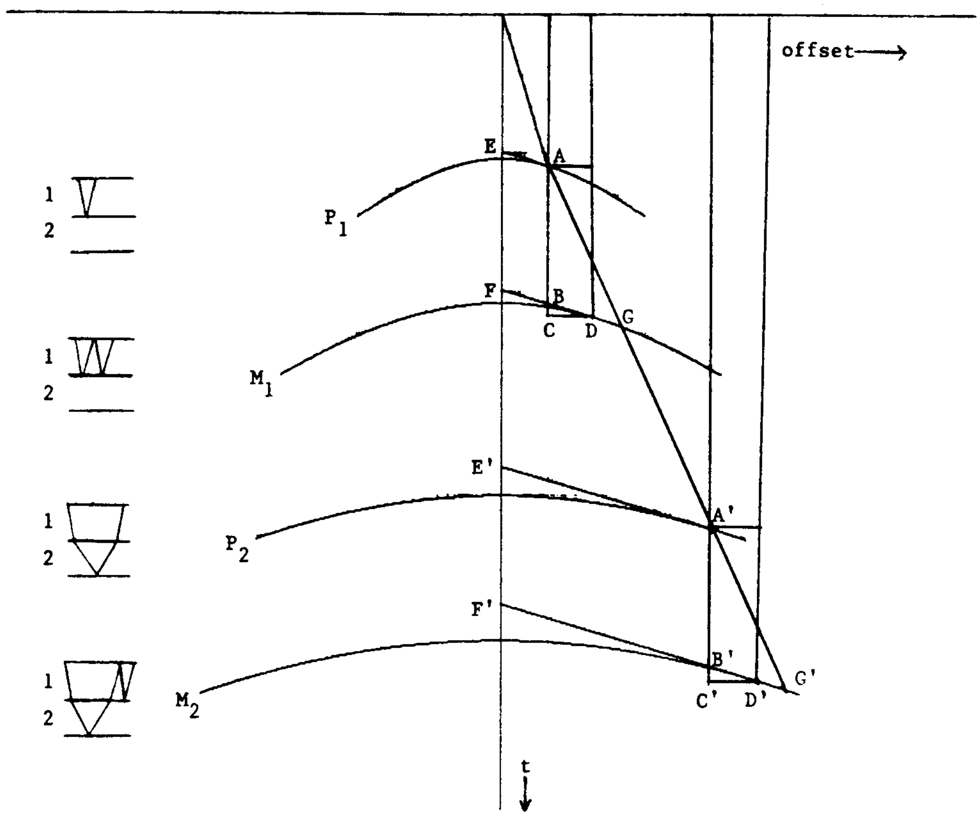

FIG. (3.8.1). A two layer model with $v_2 > v_1$. Note that the time separation, P_1M_1 is not equal to the separation of P_2M_2 on the radial trace ($|AG| \neq |A'G'|$). Nevertheless, an ideal slant stack preserves a uniform reverberation period (i.e. - $|EF| = |E'F'|$).

The general dereverberation operator is too expensive to implement except in certain special cases - the most important being the limit of zero dip. The three most popular predictive methods in industry - radial trace, zero dip F-K prediction, and slant stack prediction all make the zero dip assumption. The methods differ in their assumptions about sediment velocity, and seafloor and ghost responses.

Another common approximation to the full dereverberation operator is to simulate the response of only one field below the seafloor. In theory, this removes all of the water bottom multiples and n of the $n+1$ components of an n'th order pegleg multiple - for only half the cost of the full job.

REFERENCES

Clayton, R.W. and Stolt, R.H. (1981), A Born-WKBJ Inversion Method for Acoustic Reflection Data, Geophysics Vol. 46, No. 11, pp. 1559-1567.

Estevez, R.J. (1977), Wide-Angle Diffracted Multiple Reflections, Stanford University Ph.D. Dissertation

Fourmann, Lerat, and Tariel (1979), Talk given at E.A.E.G. meeting - Dublin.

Goupillaud, P.L. (1965), An Approach to Inverse Filtering of Near Surface Layer Effects from Seismic Records, Geophysics 26, pp. 754-760.

Riley, D.C. and Claerbout, J.F. (1976), 2-D Multiple Reflections, Geophysics 41, pp. 592-620.

Sherwood, J.W.C. and Trorey, A.W. (1965), Minimum Phase and Related Properties of a Horizontal Stratified Absorptive Earth Due to Plane Acoustic Waves, Geophysics 30, pp. 191-197.

Taner, M.T. (1980), Long-Period Sea-Floor Multiples and Their Suppression, Geophysical Prospecting 28, pp. 30-48.

Treitel, S. and Robinson, E.A. (1966), Seismic Wave Propagation in Layered Media in Terms of Communication Theory, Geophysics 31, pp.17-32.

Yilmaz,O. (1979), Ph.D. Thesis, Stanford University

Yilmaz,O. and Claerbout,J.F. (1980), Pre-Stack Partial Migration, Geophysics 45, pp. 1753-1779

3.A A Scattering Theory Interpretation

For those favoring the inverse scattering approach to seismic inversion, the dereverberation procedure of Section 3.3 may be interpreted as follows.

We assume that the Lippmann-Schwinger expansion (Clayton and Stolt, 1981) for the observed data, D, can be approximated by:

$$D = \sum_{i=0} \sum_{j=0} (G_0 \hat{V} G_0 \overline{V})^i \, GVG (\overline{V} G_0 \hat{V} G_0)^j \qquad (3.A.1)$$

The term "GVG" in the centre of the expansion denotes the primary observations at the sea surface. $\overline{V} = -1$ is the free surface potential. G_0 is the constant velocity Green's function for propagation in water. The "0" subscript emphasizes that - unlike G - this is a *known* Green's function. $\hat{V}$ is a potential which is assumed to have support only in the vicinity of the seafloor. It is estimated from the data by solving the problem

$$\min_{\hat{V}} ||DG_0^{-1} - D\bar{V}G_0\hat{V}||^2 \quad (3.A.2)$$

Now define .

$$D_1 = (DG_0^{-1} - D\bar{V}G_0\hat{V})G_0 \quad (3.A.3)$$

Note that if $\hat{V}$ has been correctly estimated, then

$$D_1 = \sum_i (G_0\hat{V}G_0\bar{V})^i GVG \quad (3.A.4)$$

We now find

$$D_2 = G_0(G_0^{-1}D_1 - \hat{V}G_0\bar{V}D_1) = (1 - G_0\hat{V}G_0\bar{V})D_1 \quad (3.A.5)$$

$$= GVG$$